Summer ozone variation in North China based on satellite and site observations

Lihua Zhou[1], Jing Zhang[1], Hui Wang[1], Wenhao Xue[1], Xiaohui Zheng[1], and Siguang Zhu[2]

[1]College of Global Change and Earth System Science, Beijing Normal University, Beijing, China

5   [2] Collaborative Innovation Center on Forecast and Evaluation of Meteorological Disasters/Key Laboratory of Meteorological Disaster of Ministry of Education, Nanjing University of Information Science and Technology, Nanjing, China

Correspondence to: Jing Zhang (jingzhang@bnu.edu.cn)

Abstract. Compared with other regions, air pollution in North China is very serious, especially its levels of fine particulate matter, which are closely associated with the concentrations of polluting gases, such as nitrogen oxides, sulfur oxides, organic

10   gases, and ozone. Fine particle pollution has been studied in-depth, but there is less known about ozone. This paper focuses on the interannual variability of tropospheric ozone in North China and identifies its influential factors. Our analysis relies on satellite observations (ozone, nitrogen dioxide, sulfur dioxide, carbon monoxide and formaldehyde concentrations) and near-surface data (carbon monoxide, sulfur dioxide, nitrogen dioxide, fine particulate concentrations, temperature, and humidity). Studies have shown that the tropospheric ozone column in North China has been at a high level for the past 3 years, with the

15   similar time series for temperature and formaldehyde. However, trends in ozone are opposite to those of sulfur dioxide and nitrogen dioxide over this 3-year period. This indicates that the increase in ozone in North China was mainly caused by the increase in temperature and an increase in organic gas content, rather than by nitrogen oxides. Over both temporal and spatial scales, the production rate of ozone appears to be most sensitive to temperature change, as ground observations in Beijing have suggested.

20   **1 Introduction**

Ozone (O_3) in the atmosphere is mostly distributed within the stratosphere, where it absorbs ultraviolet radiation and maintains atmospheric temperature. Consequently, the O_3 content in the troposphere is relatively small, being about ten times less. However, tropospheric O_3 has more direct and important impacts on human health and ecosystems. In recent years, North China has experienced severe air pollution, especially related to fine particles of pollution gases.

25   A large range in spatial distribution and long-term temporal changes of O_3 are observed in satellite data. Typically, O_3 pollution is closely related to other air pollution components, such as NO_x and volatile organic compounds (VOCs) (Sillman et al., 2003), as well as temperature and humidity. Although previous studies have mostly been based on a case study of the O_3–VOC–NO_x system sensitivity, there are few large scale studies of range or change (Carrillo-Torres et al., 2017). In this study, the horizontal transport of O_3 was not considered. We only considered vertical transport and photochemical reactions because in summer

Atmospheric
Chemistry
and Physics
Discussions

these are the two major contributors to tropospheric O_3 under NO_x-limited conditions (Liu et al., 2010). Specific O_3 pollution incidents have received much attention and analysis, although long-term studies based on atmospheric compositions obtained from satellite observations are more likely to show a wide range of macro changes. Numerous studies have shown that Ozone Monitoring Instrument (OMI) observations are reliable for assessment of sources, as well as regional and global

5   characterization of spatiotemporal variability of O_3 (Krotkov et al., 2016; Boersma et al., 2009; Boersma et al., 2008). Such data are worthwhile, as there are still some differences between the atmospheric conditions provided by the laboratory and the actual atmosphere. Chemical reactions in the atmosphere are complex, suggesting we need to visualize the relationship between the concentration of O_3 and other parameters. Therefore, we introduce temporal and spatial distributions of tropospheric O_3 sect. 3.1; sect. 3.2 discusses temporal and spatial distributions of other components; while sect. 3.3 describes relationships

10   between O_3 and other factors based on ground observations.

2 Data and methods

Tropospheric O_3, sulfur dioxide (SO_2), nitrogen dioxide (NO_2), and formaldehyde (HCHO) data are from the OMI aboard the EOS Aura spacecraft, launched 15 July 2004. Detailed data descriptions are provided in the OMI Data User's Guide and references therein (Zhou et al., 2017; Huang et al., 2015; Zhu et al., 2014; Gray et al., 2011). The daily retrieved total column

15   carbon monoxide (CO) is from Measurement of Pollution in the Troposphere (MOPITT), available at https://terra.nasa.gov/about/terra-instruments/mopitt (Heald et al., 2003). The resolution of these data is $360° \times 180°$ (units: mol/cm^2). Ground measurements for daily SO_2, NO_2, 8-h O_3 data and other near-ground gas data were obtained by averaging hourly data recorded at an Environmental Protection Station. Such air quality data have been recorded in most cities since 2013.

20   Daily average humidity and daily maximum temperature data were retrieved from the China Meteorological Administration Meteorological Data Center (http://data.cma.cn/data/). Grid data for the Monthly Mean Maximum Temperature at 2 m were obtained for North China from National Centers for Environmental Prediction (NCEP)/National Center for Atmospheric Research (NCAR) Reanalysis. Daily surface solar radiation downwards data were retrieved from the European Centre for Medium-Range Weather Forecasts (ECMWF). Monthly values were derived from the average of the daily value in each grid,

25   with a spatial resolution $0.75° \times 0.75°$. The study area, located in North China, is shown in Fig. 1. Our statistical information reflects averages of the grid points within the study area. Summer was selected as the study period, because it is the peak time for O_3 pollution in North China.

3 Results and Discussion

Atmospheric
Chemistry
and Physics
Discussions

3.1 Temporal and spatial distribution of tropospheric ozone

Figure 2 shows the monthly average O_3 distributions for the study area; these statistics cover the period from 2005 to 2016. North China is situated within the monsoon area of East Asia. The dominant airflow in winter is a dry cold northwest airstream originating from Siberia, while the dominant airflow in summer is a southeast airstream from warm and humid air masses over

5 the oceanic/coastal sea areas. As a result, the region's temperature and humidity are closely linked to season. Figure 2 shows that the distribution of O_3 is also closely related to season. Throughout the year, O_3 levels are lowest in the winter (December/January data), with highest levels in summer (June to August). Spring and autumn are transitional periods. The most ozone-intense period is July. This pattern is consistent with the seasonal distributions of temperature. July O_3 levels rose from 2005 to 2016, indicating that O_3 levels in North China are continuing to rise annually, following a longer-term trend with

10 values rising from 44.9 DU in 2006 to 52.6 DU in 2015. This trend is not apparent in winter. Table 1 lists the percentage of tropospheric O_3 per month from 2005 to 2016. These data confirm that the lowest O_3 levels are in January. For example, lowest O_3 levels in January 2006 accounted for only 5.65 % of annual amounts. Similar low values are often recorded in the December to February period, for example, levels accounted for 5.5% and 5.87 % of total amounts in February 2012 and December 2015. In contrast, levels in July 2016 accounted for 11.91 % of the whole year. Because of the increase in O_3 pollution incidents in

15 North China, now occurring during most summers, we focused our study on the summer period. In addition to O_3 distributions, we also discuss several other relevant pollutant gases and meteorological factors. Their potential to affect O_3 is analyzed to evaluate their various contributions to its spatial and temporal changes in O_3 distribution.

3.2 Temporal and spatial distributions of other components

3.2.1 Nitrogen dioxide

20 There are many types of nitrogen oxides (NO_x), several of them causing air pollution, especially nitric oxide (NO) and NO_2 (Brown et al., 2003; Foy et al., 2015). Except for NO_2 , most nitrogen oxides are extremely unstable. Under intense light, moisture or heat, they are converted into NO_2 (or NO, which in turn is converted into NO_2). Therefore, the nitrogen oxides in the atmosphere are mainly these two species, having a final form of NO_2. Therefore, over long periods, the amount of NO_2 and the total amount of nitrogen oxides are basically the same. According to previous research, there is a positive correlation

25 between atmospheric NO_x and O_3 concentrations (Scholz and Rabl, 2006). The formation of tropospheric O_3 requires a series of complex chemical reactions. NO and NO_2 act as catalysts, yielding the final chemical reaction equation: $O + O_2 \rightarrow O_3$, $\frac{[NO_2]}{[NO]} \propto [O_3]$ (Shon et al., 2008). According to satellite observations, NO_2 pollution in North China is more serious than in adjacent areas (Gu et al., 2014). The distributions of this pollution and northern industrial areas are well correlated. Annual trends in NO_2 are shown in Fig. 3. Over the past 12 years, highest peaks occurred in 2011, reaching 6.97 DU in June, 6.15 DU

30 in July, and 6.14 DU in August. In July, during the period 2005-2011, NO_2 concentrations showed a downward trend from

Atmospheric
Chemistry
and Physics
Discussions

2011 to 2016, as did concentrations in June and August. However, in July, trends in NO_2 and O_3 are not consistent. Therefore, the increase in O_3 over this period is not caused by an increase in nitrogen oxides.

3.2.2 Tropospheric sulfur dioxide

O_3 and SO_2 participate in photochemical reactions (Xie et al., 2005). Oxidation of SO_2 by O_3 in the presence of water forms

5   sulfate (Ullerstam et al., 2002). O_3 has a clear impact on SO_2 levels. We conclude that the reduction in SO_2 content may reflect an increase in atmospheric oxidants and a reduction in sulfide emissions. Enhanced oxidation properties of the atmosphere, related to increasing O_3 content, would increase the sinks of SO_2. The annual trend of SO_2 in North China is shown in Fig. 4. Quantitative calculations indicate that the overall trend is downward from 2007 to 2011. In July, the average content of SO_2 decreased by 43.2 % compared with 2005 values, while June values decreased by 49.1 %, and August values by 43.6 %.

10   ### 3.2.3 Tropospheric carbon monoxide

CO emission from biomass burning was estimated by fire counts (Duncan et al., 2003). The diffusion and migration of CO in the atmosphere is controlled by wind speed (Liu et al., 2003). The solubility of CO in water is very low, and the effect of removing it from the air through wet deposition is not significant. The reaction between CO and oxygen yields: $CO+2O_2{\rightarrow}CO_2+O_3$ (Jin, 2008). When the concentration of NO is high, one molecule of CO produces one molecule of O_3

15   (Heald et al., 2003). When the concentration of NO is low, there is no increase in O_3; there may even be a loss of O_3. In contaminated areas, CO is one of the important precursors to photochemical production of O_3. There is a positive correlation between vertical profiles of O_3 and CO (Fishman and Seiler, 1983; Choi et al., 2017), where the main fluctuations in concentrations are similar. The positive correlation between CO and O_3 suggests that tropospheric O_3 is mainly derived from photochemical processes (Tang et al., 2006; Suthawaree et al., 2008; Chin et al., 1994). The spatial distribution of CO is

20   basically like those of NO_2 and SO_2, all of which have elevated levels in North China. However, interannual trends of CO did not show a clear downward trend. This indicates there is no marked reduction in CO emissions over the study period.

3.2.4 Summer ozone concentrations and its relationship to other factors

The order of magnitude of each component in the atmosphere varies greatly and is typically normalized for ease of comparison (Ji et al., 2016). The standardization method used in this study involved normalizing to [0, 1]: $c' = \frac{c_i - c_{min}}{c_{max} - c_{min}}$, where c_i is

25   the input data, c_{min} and c_{max} are the largest and the smallest values in the series (Karanwal et al., 2010; Patel and Shah, 2015). Figure 6 shows temporal trends of various parameters (formaldehyde, temperature and surface solar radiation downwards) in July throughout North China. To compare these parameters, their time series were normalized. Since 2010, the trends in O_3 and temperature have been consistent. Meanwhile, HCHO content is positively correlated with VOC content, suggesting these has been consistent changes in all VOC species (Seinfeld and Pandis, 2006). Over the past 12 years, HCHO content has

increased, with a slight decrease following 2012. We conclude that although the concentration of nitrogen oxides decreased over this period, the concentration of O_3 did not decrease because VOCs have continued to increase (Duncan et al., 2010). Clearly, temperature and solar radiation are also important factors (Tang et al., 2006).

3.3 The relationships among ozone concentration and other factors from ground observations

5   In cities, there are many components that co-occur with O_3. Whether there is chemical correlation between these species is investigated herein. Figure 7 displays the correspondence between O_3 content and several other components in Beijing during summer periods of 2013-2016. Clearly, precursor species and meteorological factors affect O_3 concentrations, including temperature, humidity, and solar radiation levels. Herein, we have selected two factors to discuss in detail.

Clearly, CO contributes to the formation of O_3. But there are other atmospheric components, such as fine particulate matter

10   $PM_{2.5}$ (Fig. 7a) that may play a role. As the concentration of fine particles has increased, O_3 concentration also has rapidly increased. Typically, when the concentration of CO is stable, O_3 concentration rises rapidly as SO_2 concentrations increase. However, as discussed in sect. 3.2.2, SO_2 concentration declines in July, suggesting that any increase in O_3 in July is not caused by the decrease in SO_2. When the mass ratio of CO and NO_2 are close to 1/20, O_3 concentrations reach a peak. Meanwhile, when relative humidity reaches 40 %-60 %, CO concentration is greater than 2 μg m^{-3} and NO_2 concentration is greater than

15   40 μg m^{-3}, the O_3 concentration also peaks. However, the effect of temperature is most pronounced, showing a strong positive correlation with O_3 levels (Fig. 7e) (Duncan et al., 2009).

4 Conclusions

Based long-term statistics, the tropospheric O_3 content of North China is highest in summer (from June to August), accounting for about 33 % of annual amounts, with highest levels in July (Table 1). Tropospheric O_3 column concentrations for July are

20   increasing annually in North China. Near the ground, such periods have been associated with increasing O_3 pollution incidents. In contrast, the winter period (from December to February) has the lowest O_3 content, accounting for about 18 % of the whole year.

Here, we analyzed temporal and spatial changes of several key atmospheric components to evaluate their impact on O_3 formation. Changes in NO_2, SO_2, and CO were not consistent with changes in O_3 levels in July. Acid gas emissions (NO_2 and

25   SO_2) decreased annually, while O_3 has been increasing annually, suggesting that NO_2 and SO_2 are not causing O_3 pollution to increase. Similarly, there was no obvious increase related to levels of CO. One of the main uncertainties linked to O_3 formation is the impact of the emission of organic gases. We considered both CO and HCHO in this study. The impact of reductions of CO was not obvious on O_3 levels, which appear to maintain relatively stable levels. HCHO levels observed by satellite show greater fluctuation and are more volatile over this time. However, it is not certain that CO or HCHO are causing the increase

30   in summer O_3 in North China in recent years.

Another parameter to consider is rising temperature. The increase in temperature in July under current climatic conditions is the cause of enhanced pollution related to photochemical reactions. The effect of temperature on the formation of O_3 is greater than humidity, although low humidity and very high temperature are not conducive to the formation of O_3 pollution. In sunny weather, temperatures closely approximate solar radiation levels, triggering photochemical reactions which produce O_3.

5   However, this process is weakened by rainy or cloudy days. In July 2016, temperature and radiation both declined on average. However, O_3 content did not drop. This may be related to levels of fine particulate pollution in the air. We found a strong co-occurrence of O_3 and fine particle contamination in this region. Therefore, O_3 pollution cannot be separated from hazy production. This also explains why the concentration of O_3 is higher than other climatically warm areas in North China in summer, given that the average $PM_{2.5}$ in Beijing in July was 61 µg m^{-3} in 2015, and 69 µg m^{-3} in 2016.

10   *Author contributions.* Lihua Zhou collected and analyzed the data. Lihua Zhou and Jing Zhang participated in the design of the study and wrote the paper. All authors discussed the research.

Competing interests. The authors declare that they have no conflict of interest.

15   **References**

Boersma, K. F., Jacob, D. J., Eskes, H. J., Pinder, R. W., Wang, J., and Ronald, J. A.: Intercomparison of SCIAMACHY and OMI tropospheric NO_2 columns: Observing the diurnal evolution of chemistry and emissions from space, Journal of Geophysical Research Atmospheres, 113(D16), D16S26, 2008.

Boersma, K. F., Jacob, D. J., Trainic, M., Rudich, Y., Desmedt, I., Dirksen, R., and Eskes, H. J.: Validation of urban NO_2

20   concentrations and their diurnal and seasonal variations observed from the SCIAMACHY and OMI sensors using in situ surface measurements in Israeli cities, Atmospheric Chemistry & Physics, 9(12), 3867-3879, 2009.

Brown, S. S., Stark, H., Ryerson, T. B., Williams, E. J., Jr, D. K. N., Trainer, M., Fehsenfeld, F. C., and Ravishankara, A. R.: Nitrogen oxides in the nocturnal boundary layer: Simultaneous in situ measurements of NO_3, N_2O_5, NO_2, NO, and O_3, Journal of Geophysical Research Atmospheres, 108(D9), 4299, 2003.

25   Carrillo-Torres, E. R., Hernández-Paniagua, I. Y., and Mendoza, A.: Use of Combined Observational- and Model-Derived Photochemical Indicators to Assess the O_3-NOx-VOC System Sensitivity in Urban Areas, Atmosphere, 8(2), 22, 2017.

Chin, M., Jacob, D. J., Munger, J. W., Parrish, D. D., and Doddridge, B. G.: Relationship of ozone and carbon monoxide over North America, Journal of Geophysical Research Atmospheres, 99(D7), 14565-14573, 1994.

Choi, H. D., Liu, H., Crawford, J. H., Considine, D. B., Allen, D. J., Duncan, B. N., Horowitz, L. W., Rodriguez, J. M., Strahan,

30   S. E., Zhang, L., Liu, X., Damon, M. R., and Steenrod, S. D.: Global O_3-CO correlations in a chemistry and transport model

Atmospheric
Chemistry
and Physics
Discussions

during july-august: evaluation with tes satellite observations and sensitivity to input meteorological data and emissions, Atmospheric Chemistry & Physics, 17, 1-65, 2017.

Duncan, B. N., Martin, R. V., Staudt, A. C., Yevich, R., and Logan, J. A.: Interannual and seasonal variability of biomass burning emissions constrained by satellite observations, Journal of Geophysical Research Atmospheres, 108(D2), ACH 1-22, 2003.

Duncan, B. N., Yoshida, Y., Damon, M. R., Douglass, A. R., and Witte, J. C.: Temperature dependence of factors controlling isoprene emissions, Geophysical Research Letters, 36(5), L05813, 2009.

Duncan, B. N., Yoshida, Y., Olson, J. R., Sillman, S., Martin R. V., Lamsal, L., Hu, Y., Pickering, K. E., Retscher, C.,Allen, D. J., Crawford J. H.: Application of omi observations to a space-based indicator of no and voc controls on surface ozone formation, Atmospheric Environment, 44(18), 2213-2223, 2010.

Fishman, J., and Seiler, W.: Correlative nature of ozone and carbon monoxide in the troposphere: Implications for the tropospheric ozone budget, Journal of Geophysical Research Oceans, 88(C6), 3662–3670, 1983.

Foy, B. D., Lu, Z., Streets, D. G., Lamsal, L. N., and Duncan, B. N.: Estimates of power plant NO_x, emissions and lifetimes from omi NO_2 satellite retrievals, Atmospheric Environment, 116, 1-11, 2015.

Gray, B. A., Wang, Y., Gu, D., Bandy, A., Mauldin, L., Clarke, A., Alexander, B., and Davis, D. D.: Sources, transport, and sinks of SO_2, over the equatorial pacific during the pacific atmospheric sulfur experiment, Journal of Atmospheric Chemistry, 68(1), 27-53, 2011.

Gu, D., Wang, Y., Smeltzer, C., & Boersma, K. F.: Anthropogenic emissions of nox over china: reconciling the difference of inverse modeling results using GOME-2 and omi measurements, Journal of Geophysical Research Atmospheres, 119(12), 7732–7740, 2014.

Heald, C. L., Jacob, D. J., Fiore, A. M., Emmons, L. K., Gille, J. C., Deeter, M. N., Warner, J., Edwards, D. P., Crawford, J. H., and Hamlin, A. J.: Asian outflow and trans-Pacific transport of carbon monoxide and ozone pollution: An integrated satellite, aircraft, and model perspective, Journal of Geophysical Research Atmospheres, 108(D24), ACH 25-1, 2003.

Huang, K., Zhang, X., and Lin, Y.: The "APEC Blue" phenomenon: Regional emission control effects observed from space, Atmospheric Research, 164–165, 65-75, 2015.

Ji, X., Du, S., and Wang, G.: Using Min-Max Normalization to Measure the Differences of Regional Economic Growth-A Case Study of Yulin Area,Shanxi Province, Economy & Management, 30(03), 54-56, 2016.

Jin, S.: The Characteristics Study of Surface Ozone and Carbon Monoxide Concentrationat Waliguanin Qinghai, Nanjing University of Information Science & Technology, 2008.

Karanwal, S., Kumar, D., and Maurya, R.: Results evaluation of max rule, min rule and product rule in score fusion multibiometric systems, International Journal on Computer Science & Engineering, 2(4), 1415-1418, 2010.

Krotkov, N. A., Mclinden, C. A., Li, C., Lamsal, L. N., Celarier, E. A., Marchenko, S. V., Swartz, W. H., Bucsela, E. J., Joiner,

Atmospheric
Chemistry
and Physics
Discussions

J., and Duncan, B. N.: Aura OMI observations of regional SO_2 and NO_2 pollution changes from 2005 to 2015, Atmospheric Chemistry & Physics, 16(7), 4605-4629, 2016.

Liu, H., Jacob, D. J., Bey, I., Yantosca, R. M., Duncan, B. N., and Sachse, G. W.: Transport pathways for asian pollution outflow over the pacific: interannual and seasonal variations, Journal of Geophysical Research: Atmospheres, 108(D20),

5   8786, 2003.

Li, Q., Jacob, D. J., Bey, I., Palmer, P. I., Duncan, B. N., Field, B. D., Martin, R. V., Fiore A. M., Yantosca, R. M., Parrish, D. D., Simmonds, P. G., and Oltmans, S. J.: Transatlantic transport of pollution and its effects on surface ozone in europe and north america, Journal of Geophysical Research, 107(D13), 4166, 2002.

Liu, X. H., Zhang, Y., Xing, J., Zhang, Q., Wang, K., Streets, D. G., Jang, C., Wang, W. X., and Hao, J. M.: Understanding of

10   regional air pollution over China using CMAQ, part II. Process analysis and sensitivity of ozone and particulate matter to precursor emissions, Atmospheric Environment, 44(30), 3719-3727, 2010.

Patel, B. H., and Shah, A. N.: Privacy Preserving in DM using min-max normalization and noise addition, International Journal of Advance Engineering and Research Development, 2(10), 90-97, 2015.

Scholz, W., and Rabl, P.: Unexpectedly low decrease of NO_2 air pollution - Correlation with ozone concentration and altered

15   exhaust emissions, 2(107), 264-269, 2006.

Seinfeld, J. H., and Pandis, S. N.: Atmospheric Chemistry and Physics: From Air Pollution to Climate Change, Wiley-Interscience, 2006.

Shon, Z. H., Madronich, S., Song, S. K., Flocke, F. M., Knapp, D. J., Anderson, R. S., Shetter, R. E., Cantrell, C. A., Hall, S. R., and Tie, X.: Characteristics of the $NO-NO_2-O_3$ system in different chemical regimes during the MIRAGE-Mex field

20   campaign, Atmospheric Chemistry & Physics & Discussions, 8(23), 7153-7164, 2008.

Sillman, S., Vautard, R., Menut, L., and Kley, D.: O_3-NOx-VOC sensitivity and NOx-VOC indicators in Paris: Results from models and Atmospheric Pollution Over the Paris Area (ESQUIF) measurements, Journal of Geophysical Research Atmospheres, 108(D17), 8563, 2003.

Suthawaree, J., Kato, S., Takami, A., Kadena, H., Toguchi, M., Yogi, K., Hatakeyama, S., and Kajii, Y.: Observation of ozone

25   and carbon monoxide at Cape Hedo, Japan: Seasonal variation and influence of long-range transport, Atmospheric Environment, 42(13), 2971-2981, 2008.

Tang, X., Zhang, Y., and Shao, M.: Atmospheric Environmental Chemistry, Higher Education Press, 2006.

Ullerstam, M., Vogt, R., Langer, S., and Ljungström, E.: The kinetics and mechanism of SO_2 oxidation by O_3 on mineral dust, Physical Chemistry Chemical Physics, 4(19), 4694-4699, 2002.

30   Xie, S., Yu, T., Zhang, Y., Zeng, L., Qi, L., and Tang, X.: Characteristics of PM10, SO_2, NO(x) and O_3 in ambient air during the dust storm period in Beijing, Science of the Total Environment, 345(1-3), 153-164, 2005.

Zhou, L., Zhang, X., Zhang, J., Zhu, S., and Meng, X.: A case study of air quality control in Beijing and the surrounding area

during the 2015 World Championships and Parade, Atmospheric and Oceanic Science Letters, 10(3), 252-260, 2017.

Zhu, L., Jacob, D. J., Mickley, L. J., Marais, E. A., Cohan, D. S., Yoshida, Y., Duncan, B. N., Abad, G. G., and Chance, K. V.: Anthropogenic emissions of highly reactive volatile organic compounds in eastern texas inferred from oversampling of satellite (OMI) measurements of hcho columns, Environmental Research Letters, 9(11), 114004, 2014

5

Figure 1: The focus area of this study is within block, as the North China area referred to in the article.
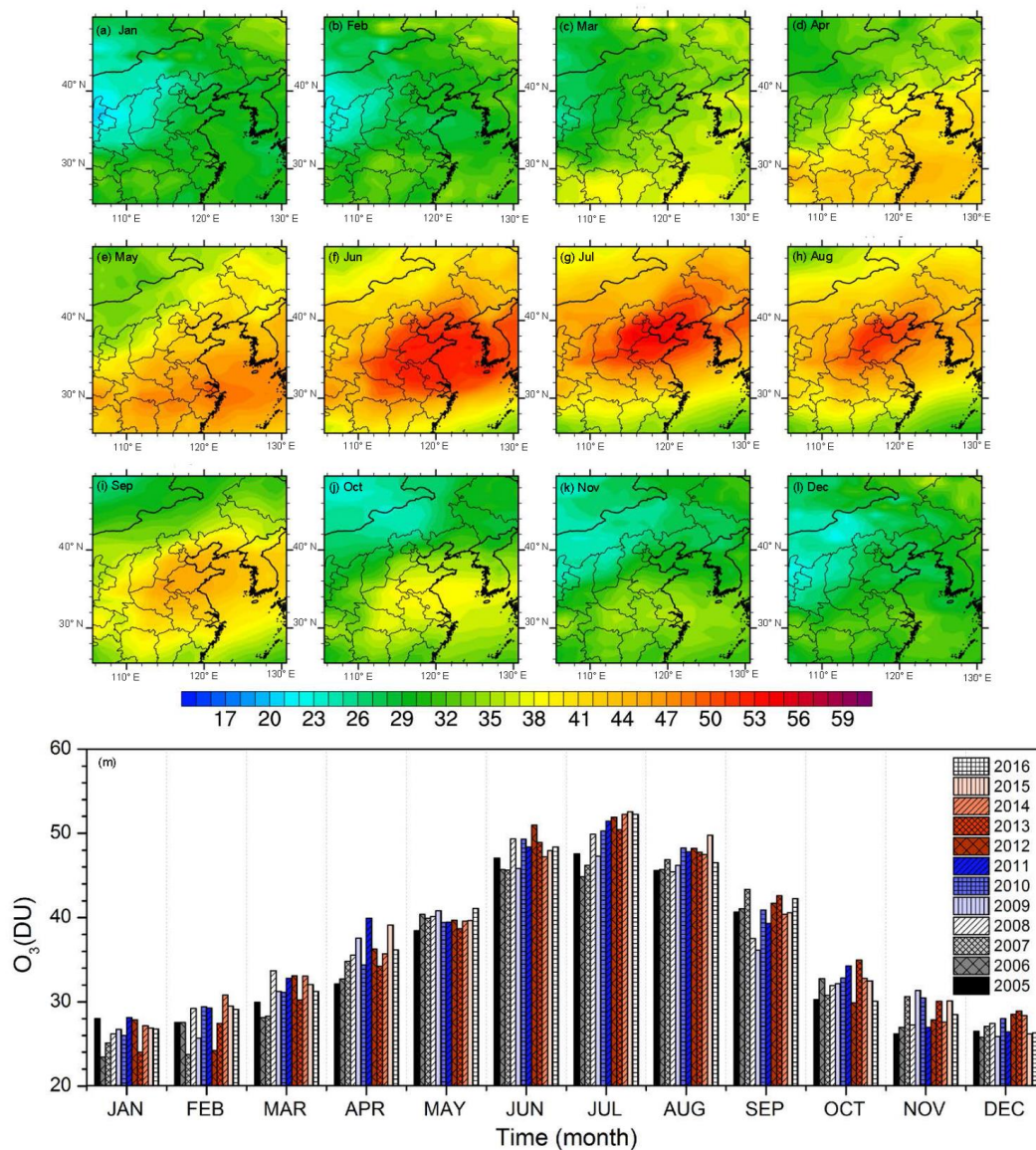
Atmospheric
Chemistry
and Physics
Discussions

Figure 2: Monthly average ozone vertical column density（VCD）distribution in the troposphere（2005 - 2016）and monthly time series of ozone in North China, as the area in the box in Figure 1 (unit: DU).

Atmospheric
Chemistry
and Physics
Discussions
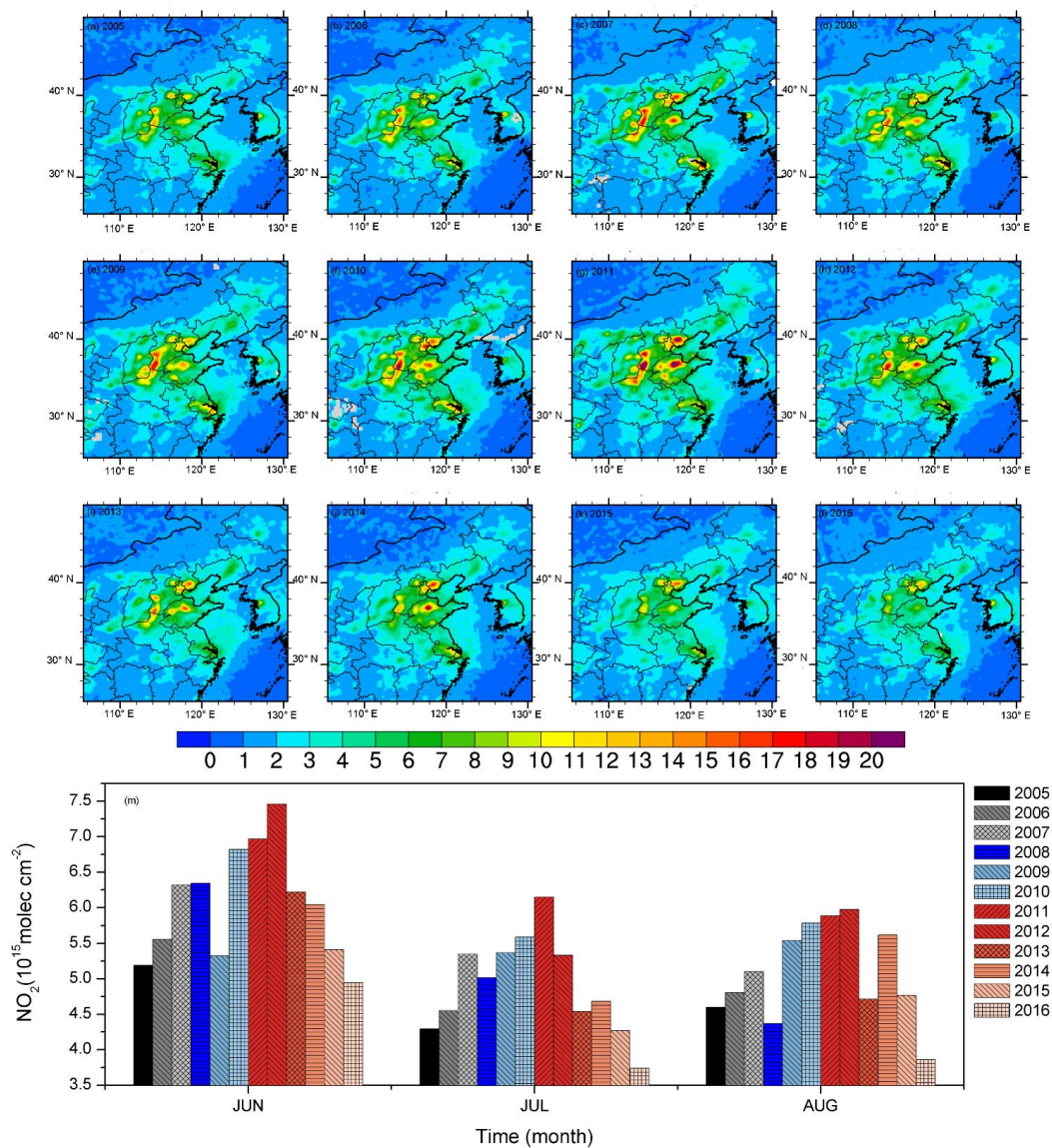

Figure 3: Average nitrogen dioxide vertical column density distribution in July（2005 - 2016）in the troposphere and summer (from June to August) time series of nitrogen dioxide in North China, as the area in the box in Figure 1 (unit: 10^{15}molec cm^{-2}).
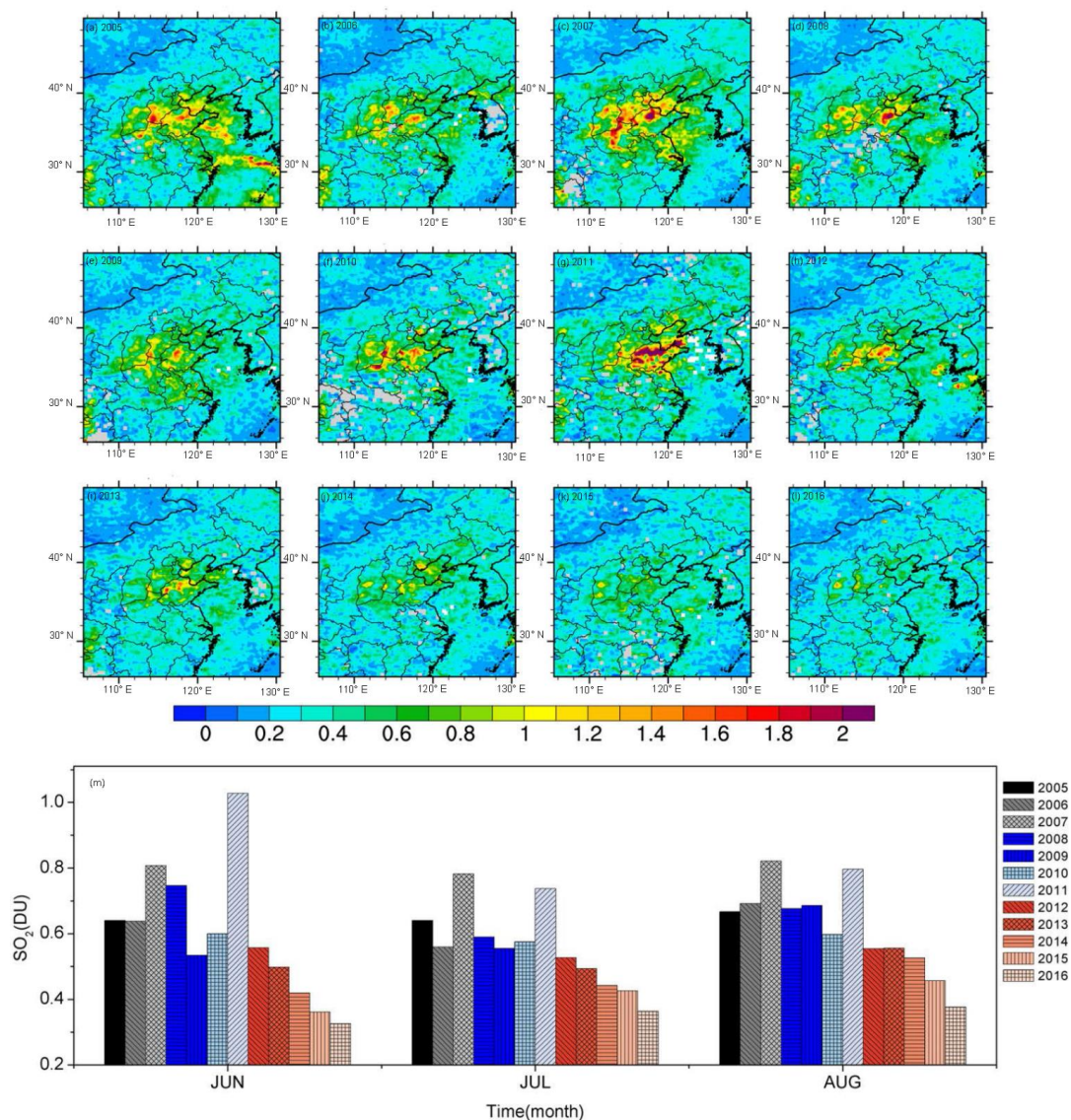
Atmospheric
Chemistry
and Physics
Discussions

Figure 4: Average sulfur dioxide column density distribution in July （2005 - 2016）in the troposphere and summer (from June to August) time series of sulfur dioxide in North China, as the area in the box in Figure 1 (unit: DU).
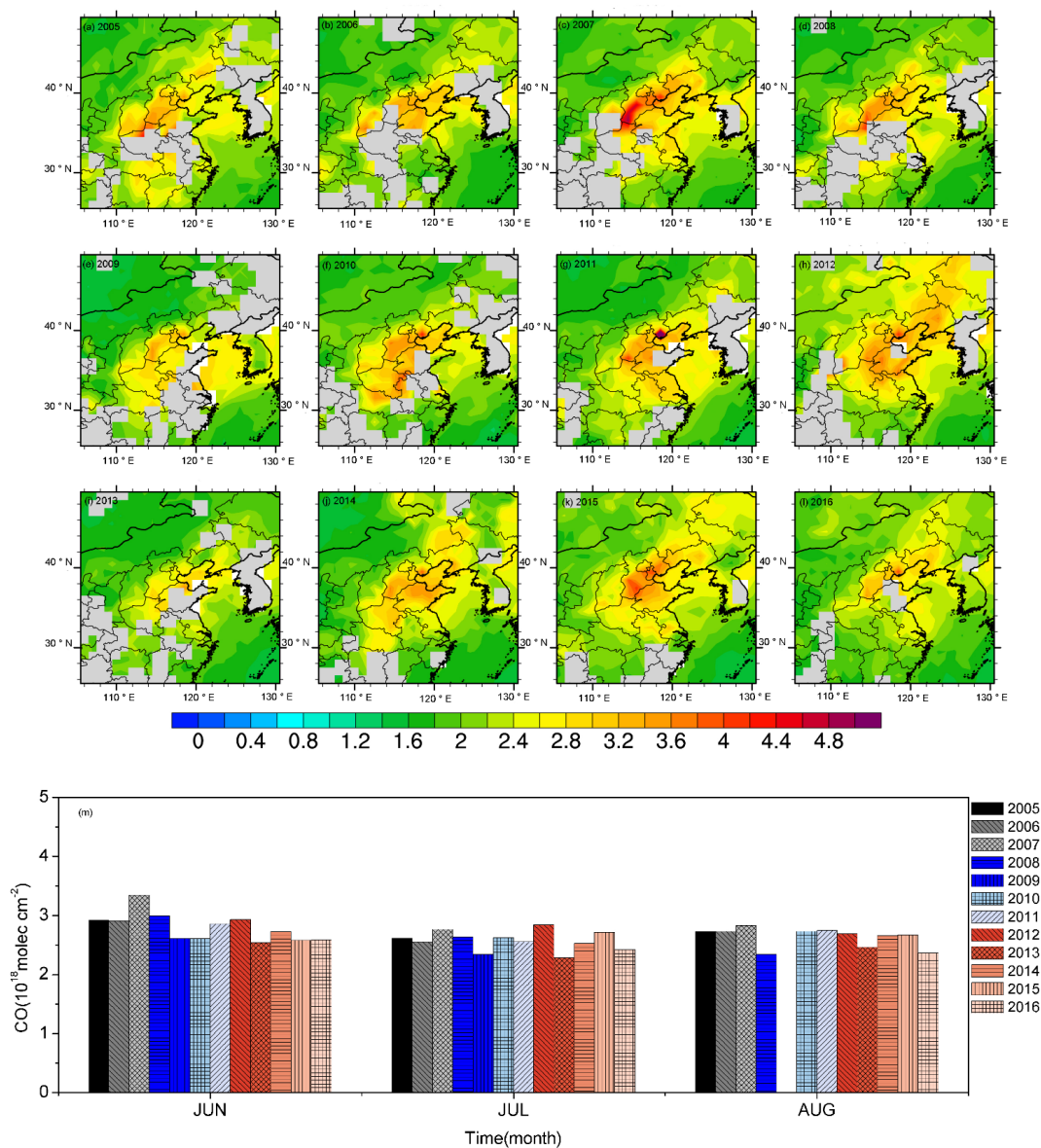
Figure 5: Average carbon monoxide column density distribution in July in the troposphere and summer (from June to August) time series of carbon monoxide (unit: 10^{18}molec cm^{-2}) in North China, as the area in the box in Figure 1.

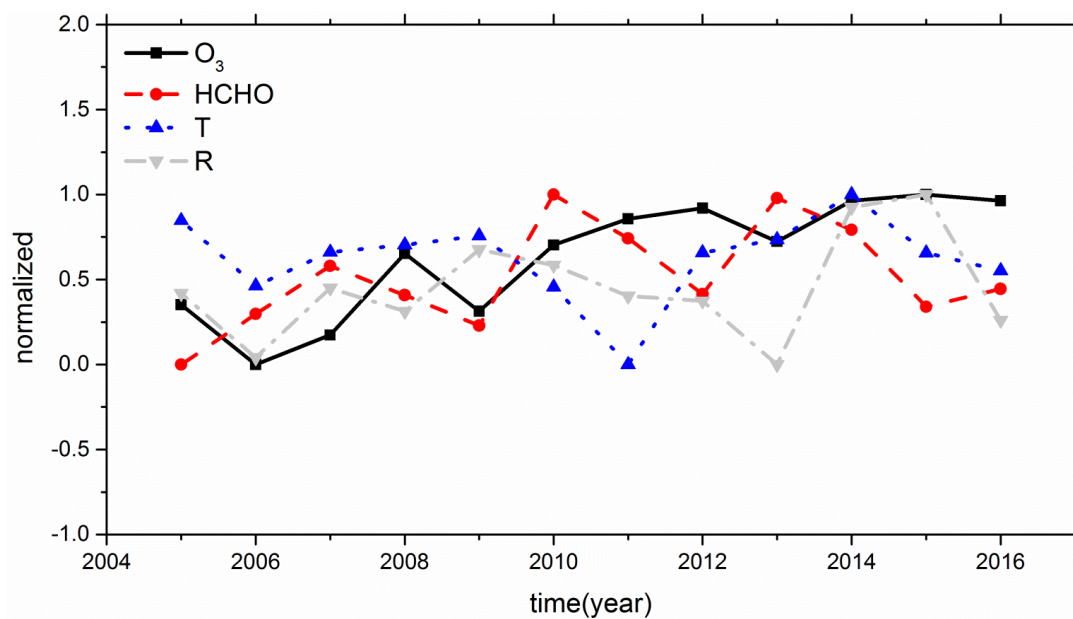Atmospheric
Chemistry
and Physics
Discussions

Figure 6: Correspondence trends standardized of ozone (O₃), formaldehyde (HCHO) and temperature (T), surface solar radiation downwards (R).
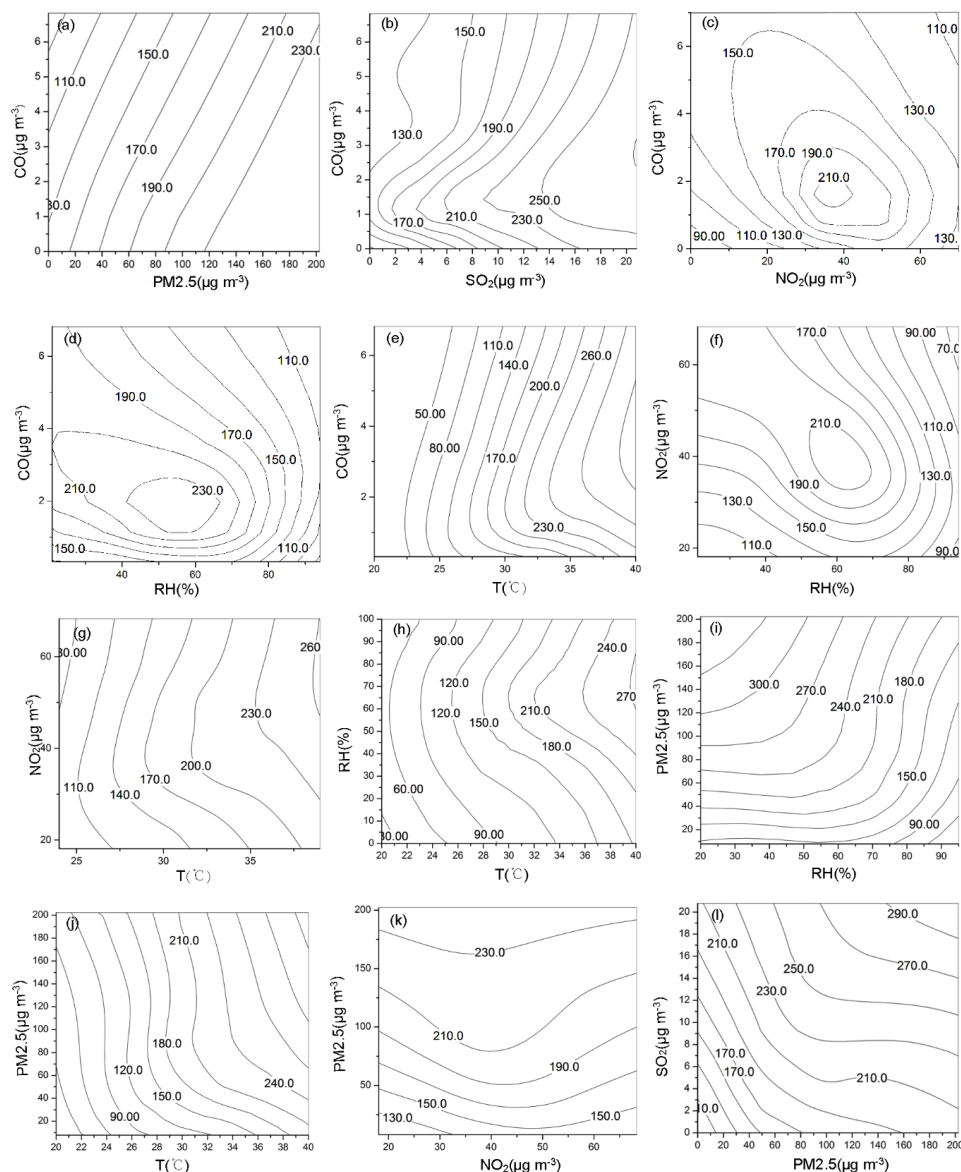
Figure 7: Correspondence between ozone content (unit: μg m⁻³) and other factors observation in Beijing during summer from 2013-2016.

Table 1: Monthly percentage of ozone content and annual content.

O₃/%	2005	2006	2007	2008	2009	2010	2011	2012	2013	2014	2015	2016
JAN	6.67	5.65	5.95	6.04	6.26	5.9	6.33	6.33	5.48	6.14	6.02	6.1
FEB	6.56	6.64	5.63	6.74	6.01	6.68	6.59	5.5	6.26	6.96	6.6	6.64
MAR	7.31	6.78	6.69	7.77	7.32	7.07	7.39	7.52	6.9	7.47	7.17	7.13
APR	7.65	7.88	8.24	8.2	8.8	7.81	8.99	8.24	7.81	8.07	8.75	8.24
MAY	9.15	9.73	9.45	9.26	9.56	8.95	8.88	9.02	8.83	8.94	8.87	9.37
JUN	11.21	11.01	10.81	11.39	10.74	11.2	10.9	11.6	11.16	10.67	10.73	11.03
JUL	11.33	10.81	10.94	11.51	11.08	11.4	11.58	11.8	11.51	11.81	11.76	11.91

AUG	10.85	11.01	11.1	10.48	10.83	11	10.76	11	10.9	10.74	11.14	10.6
SEP	9.68	9.89	10.26	8.66	8.47	9.29	8.85	9.47	9.72	9.13	9.08	9.64
OCT	7.21	7.89	7.28	7.36	7.53	7.46	7.72	6.79	7.98	7.41	7.27	6.85
NOV	6.24	6.5	7.25	6.28	7.34	6.92	6.07	6.33	6.86	6.24	6.74	6.49
DEC	6.31	6.22	6.41	6.32	6.06	6.36	5.95	6.48	6.59	6.41	5.87	6

Table 2: O_3, NO_2, SO_2, HCHO, CO based on satellite and temperature (T), surface solar radiation downwards (R) in North China.

	O_3	NO_2	SO_2	HCHO	CO	T	solar radiation
	(DU)	(10^{15}molec cm^{-2})	(DU)	(10^{15}molec cm^{-2})	(10^{18}molec cm^{-2})	(℃)	(10^6 J m^{-2})
2005	47.57	4.29	0.64	9.52	2.62	30.68	5.96
2006	44.86	4.55	0.56	10.43	2.55	28.73	5.66
2007	46.20	5.35	0.78	11.29	2.77	29.74	5.98
2008	49.89	5.02	0.59	10.77	2.64	29.95	5.88
2009	47.27	5.37	0.56	10.22	2.34	30.23	6.16
2010	50.27	5.59	0.58	12.58	2.63	28.69	6.09
2011	51.45	6.15	0.74	11.79	2.56	26.37	5.95
2012	51.93	5.33	0.53	10.79	2.84	29.72	5.92
2013	50.43	4.54	0.49	12.51	2.28	30.11	5.63
2014	52.27	4.68	0.44	11.94	2.53	31.46	6.36
2015	52.55	4.27	0.43	10.56	2.72	29.71	6.42
2016	52.27	3.74	0.36	10.88	2.42	29.18	5.84